Phosphorothioate Oligonucleotides Block the VDAC Channel

Wenzhi Tan,* Yue-Hin Loke,* C. A. Stein,† Paul Miller,‡ and Marco Colombini*
*Department of Biology, University of Maryland, College Park, Maryland 20742; †Albert Einstein-Montefiore Cancer Center, Department of Oncology, Montefiore Medical Center, Bronx, New York 10467; and ‡The Johns Hopkins University, School of Public Health, Baltimore, Maryland 21287

ABSTRACT Proapoptotic phosphorothioate oligonucleotides such as G3139 (an 18-mer) induce Bcl-2-independent apoptosis, perhaps partly via direct interaction with VDAC and reduction of metabolite flow across the mitochondrial outer membrane. Here, we analyzed the interactions at the molecular level. Ten micromolar G3139 induces rapid flickering of the VDAC conductance and, occasionally, a complete conductance drop. These phenomena occur only when VDAC is in the "open" conformation and therefore are consistent with pore blockage rather than VDAC closure. Blockage occurs preferentially from one side of the VDAC channel. It depends linearly on the [G3139] and is voltage-dependent with an effective valence of −3. The kinetics indicate at least a partial entry of G3139 into VDAC, forming an unstable bound state, which is responsible for the rapid flickering (~0.1 ms). Subsequently, a long-lived blocked state is formed. An 8-mer phosphorothioate, polydeoxythymidine, induces partial blockage of VDAC and a change in selectivity from favoring anions to favoring cations. Thus, the oligonucleotide is close to the ion stream. The phosphodiester congener of G3139 is ineffective at the concentrations used, excluding a general polyanion effect. This shows the importance of sulfur atoms. The results are consistent with a binding-induced blockage rather than a permeation block.

INTRODUCTION

VDAC is the major metabolite pathway across the mitochondrial outer membrane (1–3). It is composed of a single 30–32 kDa polypeptide chain forming a barrel-like channel (4–6) with a molecular mass cutoff at ~5 kDa for nonelectrolytes (7). In the open state, VDAC is weakly anion selective and permeable to multivalent anionic metabolites such as ADP, ATP, and NADH (8–10). At high positive or negative voltages (>25 mV), the positively-charged voltage sensor region of VDAC tends to move out of the channel, reducing the diameter of the channel from ~2.5 nm to 1.8 nm and reversing the ion selectivity (11,12). This forms the closed states of VDAC. Even though the closure of VDAC results in only a 40–60% reduction of conductance, and the size of the channel is still larger than a single ATP molecule (13), closed VDAC actually becomes impermeable to ATP (9). Thus, in addition to the channel size, the distribution of the electric charge in the channel wall is very important for controlling the flow of anionic metabolites between the cytosol and mitochondria (14).

This regulation of metabolite permeation through the mitochondrial outer membrane plays a significant role in controlling cell death and apoptosis (15). Recent studies on phosphorothioate oligonucleotides, such as G3139, have strengthened the linkage (16). Phosphorothioate oligonucleotides have each phosphodiester linkage modified such that one nonbridging oxygen is replaced by a sulfur atom. This makes the oligonucleotide resistant to nuclease action. G3139 is an 18-mer phosphorothioate oligonucleotide that is antisense to the initiation region of Bcl-2 mRNA (17). It was designed to sensitize cancer cells to chemotherapy agents by downregulating Bcl-2 levels (18,19). However, when G3139 was introduced into cells, cytochrome *c* release preceded the downregulation of Bcl-2. This and the lack of strict sequence dependence (20) indicated that another mechanism must be responsible for the proapoptotic effect of G3139. Experiments with isolated mitochondria showed that G3139 interferes with metabolite flow through VDAC, and this may partly account for the ability of G3139 to induce apoptosis (16,21).

Interactions between oligonucleotides and protein channels have been intensively studied, mainly using the α-hemolysin channel (22–24). α-Hemolysin forms a heptameric channel with a diameter of 2.6 nm (25). Unlike VDAC, the α-hemolysin channel is very asymmetric with a mushroom-like domain on one membrane surface (25). However, its channel size is very similar to the open conformation of VDAC. The permeation of oligonucleotides through α-hemolysin channels (22–24) suggests that they may enter VDAC in a similar manner. This entry may account for blockage of the VDAC channel.

In this work, we investigated the molecular basis for the interaction between phosphorothioate oligonucleotides and VDAC. We propose that partial entry of G3139 into and subsequent binding to VDAC channels account for the apparent result that G3139 induces VDAC closure.

MATERIALS AND METHODS

Planar phospholipid membrane studies

Planar phospholipid membranes were generated according to standard methods (26,27). The membrane was formed from phospholipid monolayers

Submitted January 26, 2007, and accepted for publication April 26, 2007.

Address reprint requests to Marco Colombini, Dept. of Biology, University of Maryland, College Park, MD 20742. Tel.: 301 405-6925; Fax: 301 314-9358; E-mail: colombini@umd.edu.

Editor: Tzyh-Chang Hwang.

0006-3495/07/08/1184/08 $2.00

doi: 10.1529/biophysj.107.105379

consisting of diphytanoyl phosphatidylcholine, polar extract of soybean phospholipids (both from Avanti Polar Lipids, Alabaster, AL), and cholesterol (Sigma, St. Louis, MO) in a 1:1:0.1 mass ratio.

VDAC was purified from mitochondria isolated from rat liver (5,28). A 0.1-μl aliquot of the VDAC-containing solution (2.5% Triton X100, 50 mM KCl, 10 mM Tris, 1 mM EDTA, 15% DMSO, pH 7.0) was stirred into 4–6 ml of aqueous solution containing 1.0 M KCl, 5 mM $CaCl_2$, 1 mM EDTA, and 5 mM HEPES (pH 7.2) on the *cis* side of the chamber. The *trans* side, containing the same aqueous solution, was held at virtual ground by the voltage clamp.

After a single channel insertion, a triangular voltage wave at a frequency of 3 mHz from −52 mV to +52 mV was applied to the *cis* side. The current was recorded at a rate of 100 μs per point with no filtering unless mentioned otherwise. All experiments were performed at ~23°C.

The data were analyzed using the QuB program downloaded from the web site (http://www.qub.buffalo.edu/wiki/index.php/Main_Page) of the State University of New York, Buffalo.

Ion selectivity measurements

These were performed in a similar way as above except that KCl concentration gradients (0.50 M KCl vs. 0.10 M KCl; other components are: 0.5 mM $CaCl_2$, 1 mM HEPES, pH 7.2) were used and recordings were made at 1 ms per point with 2-kHz filtering. The salt activity coefficients of 0.5 M KCl and 0.1M KCl are 0.651 and 0.770, respectively. The reversal potential was measured by a linear fit to the current-voltage curve. The ion selectivity was estimated using the Goldman-Hodgkin-Katz theory.

Oligonucleotides

G3139 was kindly donated by Dr. R. Brown, Genta (Berkeley Heights, NJ). Phosphorothioate homopolythymidine 8 or 14 nucleotides in length was synthesized using standard automated phosphoramidite chemistry on an ABI Model 3400 DRNA/RNA synthesizer. ^{3}H-1,2-benzodithiol-3-one 1,1-dioxide was used as the sulfurizing agent. The 5′-dimethoxytrityl-derivatized oligonucleotides were released form the support by treatment with 400 μl of a solution containing concentrated ammonium hydroxide and 95% ethanol (3:1 v/v) for 3.5 h at 55°C. The dimethoxytrityl derivatized oligonucleotide was dissolved in 50 mM sodium phosphate (pH 5.8), and the solution was then loaded onto a C-18 reversed-phase SEP PAK cartridge (Watters, Milford, MA). The cartridge was washed sequentially with 10% acetonitrile in 50 mM sodium phosphate buffer, water, 2% trifluoroacetic acid and water. The detritylated oligonucleotide was then eluted from the cartridge with 50% aqueous acetonitrile. The purity of the oligonucleotide was confirmed by reversed-phase HPLC.

The phosphodiester congener of G3139 was synthesized by standard automated phosphoramidite chemistry. The oligonucleotide was deprotected as described above and purified by strong anion-exchange HPLC.

RESULTS

G3139 induces complete conductance loss of VDAC

VDAC is a voltage-dependent channel. When reconstituted into planar membranes, it is open at low voltages and tends to enter low-conducting, closed states at high voltages (>25 mV) (1). There are two independent sets of closed states, one at positive and the other at negative potentials. The normal VDAC closure results in only a partial conductance loss (Fig. 1 *A*), with the remaining conductance generally between 40% and 60% of that of the open state (Fig. 2). When 10 μM G3139 was added to the *cis* side of the planar membrane (same side as the addition of VDAC), rapid flickering of VDAC conductance occurred in the millisecond time scale. However, flickering was observed only when negative voltages were applied (Fig. 1, *B* and *C*). This is consistent with the field driving the negatively charged G3139 toward the lumen of the channel. Each time-resolved conductance drop during the flickering process reaches a conductance level that is close to zero. This is clearly evident in the very long-lived events (Fig. 1 *B*).

The G3139-induced closure of VDAC is clearly different from voltage-induced closure. Although both processes are voltage dependent, the kinetic properties are quite different. G3139 induces rapid gating accompanied by long-lived closing events. Without G3139, channels close with slow kinetics. The extent of closure is much greater (Fig. 2) in the presence of G3139. This closure often represents a complete loss of conductance. This complete closure requires direct interactions between G3139 and VDAC and suggests that G3139-induced VDAC closure is distinct from the normal VDAC closing process.

The closed states of VDAC have been shown to be favored by a variety of polyanions (29). In these cases, the closure is not distinguishable from normal VDAC closure. Indeed, the evidence strongly indicates that polyanions act on the normal gating process by interacting electrostatically with the positively charged voltage sensor forming part of the wall of the aqueous pore and favoring its translocation to the membrane surface (30). However, what appears to be G3139-induced VDAC closure may actually be blockage of

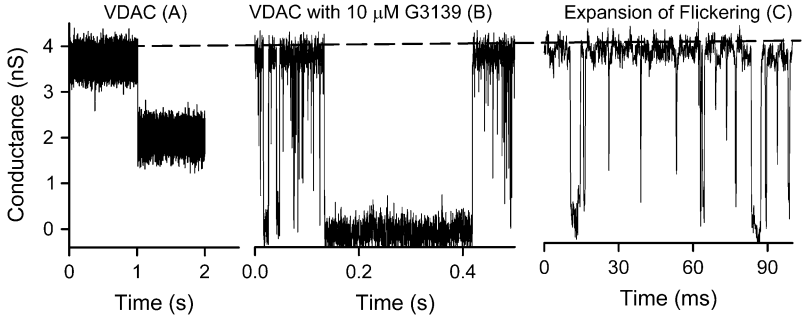

FIGURE 1 Comparison of normal VDAC closure and G3139-induced VDAC closure. These figures are from a typical experiment performed with the same single VDAC channel in response to −50 mV potential. (*A*) An example of voltage-dependent VDAC closure. (*B*) An example of G3139-induced rapid flickering and complete conductance loss of VDAC after addition of 10 μM G3139 to the same side as the VDAC addition. (*C*) An expanded scale to show G3139-induced rapid flickering of VDAC channels. These results were obtained at 0.1 ms per point and are presented without any filtering.

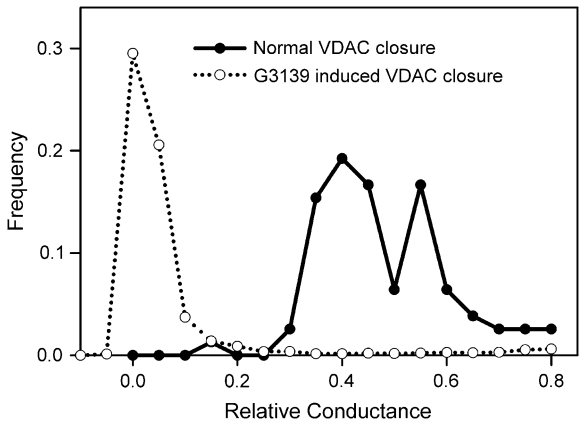

FIGURE 2 Comparison of the distribution of relative conductance of normal VDAC closure and G3139-induced VDAC closure. G3139 (10 μM) was added to the same side as the VDAC addition.

VDAC by G3139. This mechanistic distinction is reinforced by the fact that the equally charged phosphodiester congener of G3139 does not induce VDAC flickering or conductance loss (16). It also has little effect on VDAC at the concentrations used to observe the effects of G3139.

G3139 directly binds to a specific conformation of VDAC

There are several possible molecular mechanisms that could account for the observed conductance fluctuations after the addition of G3139 to VDAC channels. G3139 could induce a conformational change in VDAC resulting in the occlusion of the pore. This seems unlikely because VDAC does not normally close completely. Alternatively, G3139 could permeate through VDAC channels. Its large size and multiple negative charges might block the channel completely. Thus, the flickering would reflect the transit time of G3139. However, one could also propose that G3139 simply binds to the mouth and inner wall of the channel but does not translocate through the membrane to the other side. Long-lived occlusions would result from conformers of G3139 that bind tightly to the walls of the channel. A particularly pertinent observation that addresses this issue was made by varying the location of G3139 addition. Addition of G3139 to the same side of the membrane as VDAC addition (*cis* side) resulted in rapid flickering in ~90% of all experiments. Addition of G3139 to the opposite (*trans*) side, resulted in very little flickering (~10 events per second in 2-kHz filtering). When G3139 was added to both sides, flickering was almost exclusively observed when the *cis* side was held at a negative voltage (Fig. 3 *A*). Recall that the G3139 side must be made negative to induce flickering. The difference in the rate of flickering was quantified by measuring the time constant for channel closure (τ_{on}, or mean duration of the

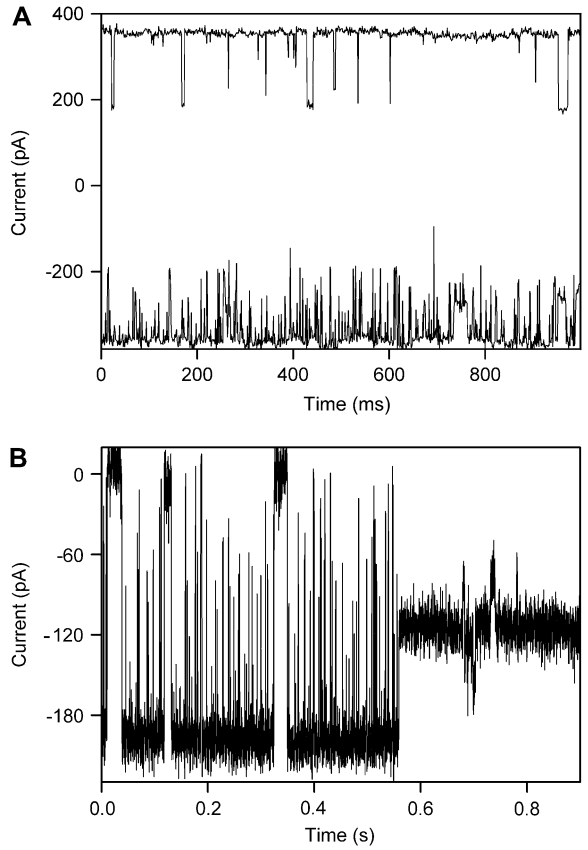

FIGURE 3 (*A*) Asymmetric flickering of VDAC induced by 40 μM G3139 present on both sides of the membrane. A voltage of −50 mV was applied to the *cis* side (*lower trace*) and to the *trans* side (*upper trace*). Two VDAC channels were present in the membrane. Recordings were made at 1 ms per point with 2-kHz filtering. (*B*) No flickering occurs when VDAC enters a normal closed state. This is a typical experiment of a single VDAC with flickering induced by 10 μM G3139 on the *cis* side. The applied voltage was −50 mV.

open state) obtained using the QuB program (see Methods). When the *cis* side was at −50 mV compared to the *trans* side, $\tau_{on} = 9.8 \pm 0.8$ ms, whereas when the *trans* side was at −50 mV compared to the *cis* side, $\tau_{on} \approx 100$ ms. This asymmetric effect could arise from a permeation blockage but is more consistent with an asymmetric binding site.

The asymmetric nature of the G3139-induced flickering reveals the asymmetric insertion of VDAC (from rat liver) into planar membranes. This observation agrees with recent findings about the asymmetric insertion pattern of VDAC from mammalian sources (31), which is different from observations made with yeast VDAC (32).

These observations also strengthen the hypothesis that G3139 specifically interacts with one area of the channel's surface. The asymmetry reveals specificity for a region of the protein. There is also specificity for the ligand because the phosphodiester congener does not induce channel blockage. The focus is clearly on the phosphorothioate backbone of G3139 because the specific sequence of bases is unimportant

(a phosphorothioate composed of just thymidine also induces flickering and full blockage, see Fig. 6). Thus, there must be some specific affinity between the phosphorothioate and some region or domain of the VDAC molecule.

The existence of a specific interacting domain on VDAC is further supported by the observation that G3139 induces flickering almost exclusively when VDAC is open. When VDAC is closed (i.e., in a low-conducting state), there is nearly no flickering (Fig. 3 *B*). This suggests some specific interactions between G3139 and the mobile region of VDAC, the voltage-sensor region (12). This is a positively charged region and thus ideal for interacting with G3139. When that positively charged region moves out of the channel (the gating process of VDAC (12)), G3139 is likely to still bind to this region, which is mostly outside the pore. This binding would not induce VDAC flickering or complete closure.

The kinetics of the interaction

Because G3139 is a charged molecule, the mechanism just presented would predict the existence of a voltage dependence to the blocking action of G3139. The QuB program was used to analyze the kinetics of the flickering events. For these experiments, G3139 was added only to the *cis* side.

Fig. 4 shows the distribution of the duration of the open and blocked states of VDAC channels under the influence of 5 μM G3139 and -40 mV. There is a single distribution of open times indicating a single open state. However, the distribution of blocked times indicates multiple blocked states. Some blocked states open quickly as evidenced by events below 1 ms (Fig. 1, *B* and *C*). However, some states are stable for very long times, resulting in events longer than 0.1 s. Clearly, these are not the same states. To simplify the analysis, one open state and two blocked states were used to model G3139-induced VDAC closure:

$$\text{open state} \underset{\leftarrow}{\overset{k}{\rightarrow}} \text{blocked state 1} \underset{\leftarrow}{\rightarrow} \text{blocked state2}\,, \qquad (1)$$

where k is the forward rate constant of the first reaction.

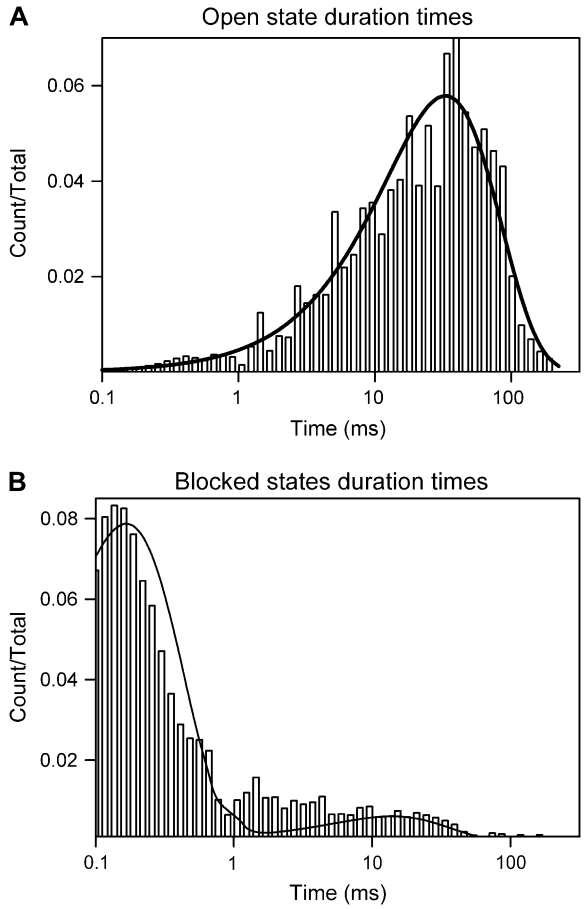

FIGURE 4 Example of the distributions of the duration of the open state (*A*) and blocked states (*B*) of G3139-induced rapid flickering of a single VDAC channel with 5 μM G3139 added to the *cis* side and -40 mV applied voltage.

Fig. 5 *A* shows a linear dependence of the rate constant, k, on the concentration of G3139. This suggests a one-to-one binding of G3139 to VDAC. The reverse rate constant is $\sim$2000–3000 s^{-1} and does not depend on the concentration of G3139. The rate constants between the two blocked states are known with less confidence because these events are very heterogeneous. Thus:

$$\text{G3139} + \text{VDAC}\,(\text{open}) \underset{k_{-1}}{\overset{k_1}{\rightleftarrows}} \text{G3139} - \text{VDAC}\,(\text{blocked1}) \underset{k_{-2}}{\overset{k_2}{\rightleftarrows}} \text{G3139} - \text{VDAC}\,(\text{blocked2}), \qquad (2)$$

Clearly, one could fit the data with more blocked states. There may be a variety of ways for G3139 to bind to VDAC: different conformers of G3139 and different ways of binding to the site on VDAC. It is possible that, with time, G3139 may adapt to the VDAC surface, increasing the strength of the interaction and thus decreasing the rate constant of dissociation. This latter process is what is modeled in Eq. 1.

where k_1 and k_{-1} are the forward and reverse rate constants of the first reaction, respectively; k_2 and k_{-2} are the forward and reverse rate constants of the second reaction, respectively.

Fig. 5 *B* shows that k_1 is voltage dependent. This is not surprising because the applied voltage changes the activation energy between the open state and the first blocked state. The energy change is equal to nFV (n is the effective valence of

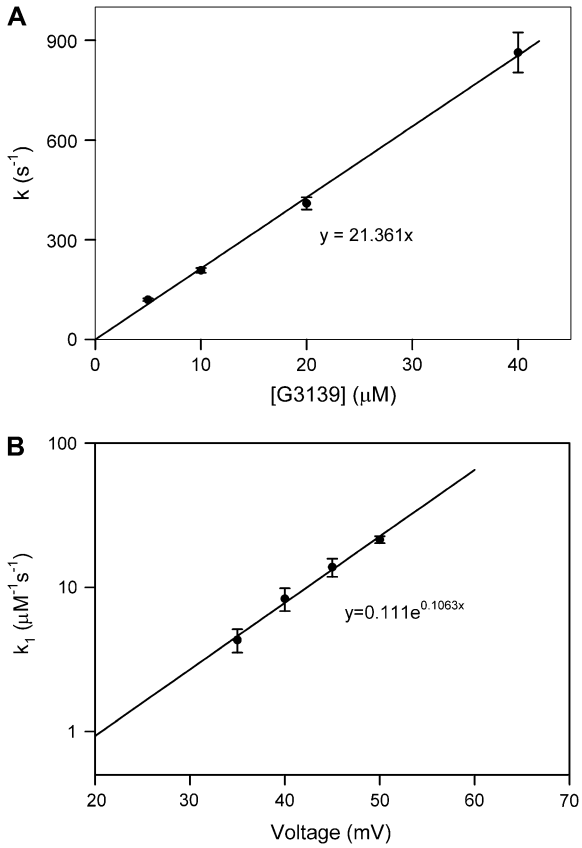

FIGURE 5 (*A*) Concentration dependence of k (see Eq. 1), the ''on'' rate constant of G3139-induced rapid flickering of a single VDAC channel at −50 mV. The error bars shown are the standard errors of a single experiment generated by QuB. The equation in the graph is the result of a linear fit. (*B*) Voltage dependence of k_1. The error bars shown are the standard errors of the slope calculated from the linear regression in the concentration dependence curve. The equation in the graph is the result of an exponential fit. These results are typical of three independent experiments.

the block, F is the Faraday constant, and V is the applied voltage). Thus, $k_1 = k_0\exp(nFV/RT)$ (k_0 is the rate constant of the same reaction with no applied voltage, R is the gas constant, and T is the temperature). Fitting the results to this equation (Fig. 5 *B*) yields an effective valence of -2.9 ± 0.1 ($n = 3$, mean ± SE) ($T = 295$ K). Even though, formally, G3139 bears a net charge of 18, experiments indicate that an oligonucleotide composed of 18 bases has a net charge of 9 because of the screening by counterions (33). In the narrow confines within the channel, the screening effect may be quite different. In any event, the voltage dependence suggests that at least part of G3139 moved through the electric field by entering the pore of the channel.

Oligonucleotide binding induces changes in selectivity

If the oligonucleotide enters the pore of the channel, its negative charge should alter the ion selectivity. However, G3139 results in a virtually complete block to ions. Thus, we tested shorter phosphorothioate oligonucleotides to achieve incomplete block and thus detect any change in ion selectivity. Phosphorothioate oligonucleotides composed entirely of the base, thymidine, are readily made, and those of comparable length are as effective on VDAC as G3139. Even the 14-mer, dT_{14} has similar abilities to induce rapid flickering and complete conductance loss of VDAC channels (Fig. 6). However, the shorter version, dT_8, only reduces the conductance to ~40–60% of that of an open VDAC channel.

The residual conductance remaining after the binding of dT_8 is cation selective ($P_K/P_{Cl} = 2$) with a reversal potential of −14 mV ± 2 mV (mean ± SE, $n = 9$). This is substantially different from the selectivity of the open VDAC channel ($P_K/P_{Cl} = 0.5$). This change in ion selectivity supports the proposed model that the flickering may be a result of the interaction of the phosphorothioate oligonucleotides and the inner wall of VDAC. dT_8 may not be long enough to fully occlude the pore. dT_{10} causes ~70–80% of full blockage, and dT_{12} causes ~80–90% of full blockage.

DISCUSSION

Attempts to make cancer cells sensitive to chemotherapy agents by knocking down the antiapoptotic protein Bcl-2 have resulted in the generation of a phosphorothioate oligonucleotide that blocks VDAC channels. This blockage does not depend on the sequence but on the phosphorothioate backbone. These molecules are the most specific VDAC blockers available to date. They will likely be useful tools to study the role of VDAC in cellular function.

The blockage of VDAC by G3139 is linearly dependent on the [G3139], indicating a 1:1 complex. It is also voltage dependent, indicating that G3139 is entering the lumen of the channel at least to some extent. dT_8, which is eight

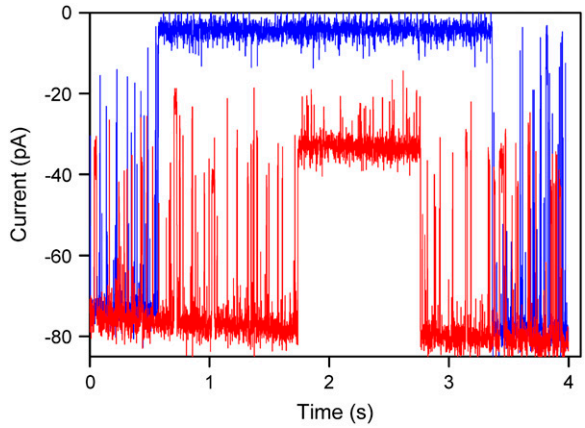

FIGURE 6 Comparison of VDAC flickering induced by phosphorothioate oligonucleotides of different lengths: dT_8 (*red trace*) and dT_{14} (*blue trace*). These were added only to the *cis* side. The voltages applied are from −49 mV to −53 mV. These are typical examples from experiments with KCl gradient (0.50 M KCl vs. 0.10 M KCl; other components are: 0.5 mM $CaCl_2$, 1 mM HEPES, pH 7.2).

nucleotides long, produces only a partial block. Full blockage requires a length of ~14 nucleotides. From a molecular dynamics simulation of a single-stranded DNA oligonucleotide inside a 2.4-nm hole (which is similar in size to the VDAC pore), the oligonucleotide has a conformation similar to that of a B-form helix, which has a distance of 0.34 nm between each base and pitch of 10 bases per turn (34). However, in the simulation the oligonucleotide had no affinity for the wall of the pore, resulting in a helix with an outside diameter on 2.0 nm. Affinity for the wall and the larger size of the VDAC pore (2.5–3 nm) should result in a helix with a greater pitch, perhaps 12. A minimum of a full turn of the helix would be needed to achieve complete block, so this explains why dT_8 achieves only an incomplete block. This also explains the almost linear increase in blockage with oligonucleotide length.

Our analysis indicates that blockage results in the effective translocation of three charges through the entire potential difference across the membrane. If the oligonucleotide were located entirely within the pore, the 18 charges would be moving an average of half way through the transmembrane potential difference. This should result in an effective valency of -9 if there is no charge screening or ~ -5 with charge screening (33). Thus, it appears that only part of the oligonucleotide is located inside the channel.

The ability of phosphorothioate oligonucleotides such as G3139 to block VDAC channels seems to arise from their ability to bind to VDAC preferentially from one side of the channel. The substantial asymmetry of the rapid flickering of conductance (Fig. 3 *A*) argues against the possibility of a permeation block, blocking in transit. VDAC is functionally and structurally rather symmetrical (1,35), forming a simple cylindrical pore. Thus, VDAC would be expected to allow oligonucleotides to permeate equally well in both directions. Single-stranded phosphodiester oligonucleotides of 30–200 bases have been shown to block the current flow through α-hemolysin (22–24) as they flow through the channel. The flickering arising from this transient blockage is asymmetric (24,36). However, this asymmetry is understandable considering the highly asymmetric structure of α-hemolysin (25). Indeed α-hemolysin is also functionally asymmetric, rectifying even in KCl solutions (36). VDAC normally shows essentially no rectification in its open state (37). Despite all this structural and functional asymmetry, α-hemolysin shows a lower level of asymmetric nucleotide block (only 6-fold) as compared to over 10-fold for VDAC exposed to G3139.

An additional difference between the G3139 block of VDAC and the observations with α-hemolysin is that much longer oligonucleotides (200 bases) must be added to α-hemolysin to obtain blockage lifetimes similar in magnitude to those reported here (23). This indicates that transit times of short oligonucleotides are too short to account for the blockage lifetimes we observe without substantial slowing of the transit by interactions with the walls of the pore.

A variety of experimental observations provide further evidence for a ''binding block'' as opposed to a permeation block:

1. Phosphodiester oligonucleotides of similar size and charge should have a similar ability to permeate VDAC channels as the phosphorothioate congener, yet these fail to cause flickering (16). This is easily explained by the binding but not the permeation model.
2. The voltage independence of the unbinding rate for the rapid flickering suggests that dissociation of the oligonucleotide is the rate-limiting step. Diffusion away from the site against the field is not rate limiting. In the permeation blockage model, unblockage should be voltage dependent. Indeed, for α-hemolysin there is an inverse voltage dependence of the poly[U]-induced blockage time (23), demonstrating that unblockage is voltage dependent.
3. The long-lived complete closure of VDAC induced by G3139 cannot be cleared by reversing the polarity of the transmembrane potential. When permeation of poly[U] through α-hemolysin results in long-lived blockage, the channels can be unblocked by reversing the sign of the potential, consistent with permeation block (23).
4. The shorter phosphorothioate oligonucleotides, such as dT_8, cause only a partial blockage. Note that the permeation blockage model would predict that the length of the oligonucleotides should determine only the blockage time (23), not the extent of blockage. Therefore, the binding of G3139 to the inner wall of VDAC and subsequent conformational changes appear to be the mechanisms for the observed flickering and complete conductance loss.

One observation that remains mysterious is the long delay between addition of G3139 and onset of flickering. The rapid flickering of conductance occurs after ~3–5 min after the addition of the phosphorothioate oligonucleotide. For G3139, which has a diffusion coefficient of 2×10^{-6} cm^2/s (33), it takes ~6 s to diffuse through a 50-μm unstirred layer next to the planar membrane. Thus, it seems that G3139 needs to adapt to VDAC before flickering occurs. Indeed, when the concentration of G3139 is increased, it takes about another 3–5 min for the flickering effect to increase. These results suggest that there might be some conformational change of G3139 after addition to the buffer solution bathing the membrane. We have tried to incubate G3139 with the buffer solution and heat it before adding it to the system, but there was still a delay. Another explanation for the delay might be a slow process of interaction between G3139 and the phospholipid membrane, which may sensitize VDAC to G3139 by changing, for example, the surface potential. Regardless of the fact that, at this stage, we don't have a good explanation for this phenomenon, this delay does not affect the proposed mechanism by which G3139 acts on VDAC.

For a VDAC channel, the transient blocked state (first step in Eq. 2) is clearly unfavorable because the k_{-1} is 2000–3000 s^{-1}. The on rate, k_1, is concentration and voltage dependent:

0.11[G3139]exp(0.11Voltage) $\mu M^{-1}s^{-1}$. At 1 μM G3139 and no applied voltage, the on rate is 0.11 s^{-1}. Thus, the equilibrium constant is 4×10^{-5} with an unfavorable free energy change of 25 kJ per mole or 10 kT. The high off rate can be compensated for by a higher on rate. A higher concentration and the application of a negative voltage obviously favor binding and make the process feasible. Rapid unbinding of G3139 from VDAC suggests the instability of the transient G3139-VDAC complex. However, the occurrence of longer complete closures clearly shows that the intermediate transient state can be stabilized. The analysis shows a slow on rate k_2 and off rate k_{-2} of the second interaction step in Eq. 2, suggesting that both of those interactions may involve some slow conformational change of VDAC and/or G3139. These structural changes make the bound state more energetically favorable and lead to complete, long-lasting VDAC closure.

Thus, the G3139-blocked VDAC channel is composed of an ''open'' VDAC channel and G3139 binding from one aqueous surface. Good candidates for surfaces forming the binding site are the positively charged voltage sensor and some adjacent region outside the pore. This explains why the lower-conducting, closed states, whose pore size was estimated to be 1.8 nm (35,38,39), show virtually no flickering despite being large enough to accommodate the oligonucleotides. However, the unfavorable net charge in the pore of the closed state of VDAC may also explain the lack of flickering. Another possible binding site is the nucleotide binding site in the inner wall of VDAC (13,40). This site may not be distinct from the voltage sensor region. The importance of phosphorothioate may be a greater affinity for the binding site on VDAC, allowing the formation of a long-lived block to metabolites. In any case, the binding of G3139 to the inner wall forms the completely blocked state, and the shorter oligonucleotides do not have the capacity to fully block the channel (Fig. 6). Obviously, the sulfur group is very important for the binding, as the phosphodiester congener does not cause VDAC flickering and complete closure (16).

Phosphorothioate oligonucleotides are, presently, the most specific inhibitors of VDAC channels. Their potency of blockage/closure of VDAC channels in isolated mitochondria is 50-fold higher than that observed for the experiments on pure VDAC reconstituted in planar membranes (as presented here). Perhaps a VDAC-associated protein or lipid increases the affinity of VDAC for the phosphorothioate. In any case, this work provides a mechanistic foundation for understanding effects in cells and organelles.

REFERENCES

1. Colombini, M. 2004. VDAC: The channel at the interface between mitochondria and the cytosol. *Mol. Cell. Biochem.* 256/257:107–115.
2. Colombini, M. 1979. A candidate for the permeability pathway of the outer mitochondrial membrane. *Nature*. 279:643–645.
3. Lee, A. C., X. Xu, E. Blachly-Dyson, M. Forte, and M. Colombini. 1998. The role of yeast VDAC genes on the permeability of the mitochondrial outer membrane. *J. Membr. Biol.* 161:173–181.
4. Song, J., C. Midson, E. Blachly-Dyson, M. Forte, and M. Colombini. 1998. The topology of VDAC as probed by biotin modification. *J. Biol. Chem.* 273:24406–24413.
5. Blachly-Dyson, E., S. Peng, M. Colombini, and M. Forte. 1990. Selectivity changes in site-directed mutants of the VDAC ion channel: structural implications. *Science*. 247:1233–1236.
6. Thomas, L., E. Blachly-Dyson, M. Colombini, and M. Forte. 1993. Mapping of residues forming the voltage sensor of the VDAC ion channel. *Proc. Natl. Acad. Sci. USA*. 90:5446–5449.
7. Colombini, M. 1980. Pore size and properties of channels from mitochondria isolated from *Neurospora crassa*. *J. Membr. Biol.* 53:79–84.
8. Hodge, T., and M. Colombini. 1997. Regulation of metabolite flux through voltage-gating of VDAC channels. *J. Membr. Biol.* 157:271–279.
9. Rostovtseva, T., and M. Colombini. 1997. VDAC channels mediate and gate the flow of ATP: implications for the regulation of mitochondrial function. *Biophys. J.* 72:1954–1962.
10. Xu, X., W. Decker, M. J. Sampson, W. J. Craigen, and M. Colombini. 1999. Mouse VDAC isoforms expressed in yeast: Channel properties and their roles in mitochondrial outer membrane permeability. *J. Membr. Biol.* 170:89–102.
11. Peng, S., E. Blachly-Dyson, M. Colombini, and M. Forte. 1992. Large scale rearrangement of protein domains is associated with voltage gating of the VDAC channel. *Biophys. J.* 62:123–135.
12. Song, J., C. Midson, E. Blachly-Dyson, M. Forte, and M. Colombini. 1998. The sensor regions of VDAC are translocated from within the membrane to the surface during the gating processes. *Biophys. J.* 74:2926–2944.
13. Rostovtseva, T. K., A. Komarov, S. M. Bezrukov, and M. Colombini. 2002. Dynamics of nucleotides in VDAC channels: structure-specific noise generation. *Biophys. J.* 82:193–205.
14. Komarov, A. G., D. Deng, W. J. Craigen, and M. Colombini. 2005. New insights into the mechanism of permeation through large channels. *Biophys. J.* 89:3950–3959.
15. Vander Heiden, M. G., N. S. Chandel, X. X. Li, P. T. Schumacker, M. Colombini, and C. B. Thompson. 2000. Outer mitochondrial membrane permeability can regulate coupled respiration and cell survival. *Proc. Natl. Acad. Sci. USA*. 97:4666–4671.
16. Lai, J. C., W. Tan, L. Benimetskaya, P. Miller, M. Colombini, and C. A. Stein. 2006. A pharmacologic target of G3139 in melonoma cells may be the mitochondrial VDAC. *Proc. Natl. Acad. Sci. USA*. 103:7494–7499.
17. Klasa, R. J., A. Gillum, R. E. Klem, and S. R. Frankel. 2002. Oblimersen Bcl-2 antisense: facilitating apoptosis in anticancer treatment. *Antisense Nucleic Acid Drug Dev.* 12:193–213.
18. Leung, S., H. Miyake, T. Zellweger, A. Tolcher, and M. E. Gleave. 2001. Synergistic chemosensitization and inhibition of progression to androgen independence by antisense Bcl-2 oligodeoxynucleotide and paclitaxel in the LNCaP prostate tumor model. *Int. J. Cancer*. 91:846–850.
19. Raffo, A., J. C. Lai, P. Miller, C. A. Stein, and L. Benimetskaya. 2004. Antisense RNA down-regulation of bcl-2 expression in DU145 prostate cancer cells does not diminish the cytostatic effects of G3139 (Oblimersen). *Clin. Cancer Res.* 10:3195–3206.
20. Lai, J. C., L. Benimetskaya, A. Khvorova, S. Wu, E. Hua, P. Miller, and C. A. Stein. 2005. Phosphorothioate oligodeoxynucleotides and G3139 induce apoptosis in 518A2 melanoma cells. *Mol. Cancer Ther.* 4:305–315.
21. Tan, W., J. C. Lai, P. Miller, C. A. Stein, and M. Colombini. 2006. Phosphorothioate oligonucleotides reduce mitochondrial outer membrane permeability to ADP. *Am. J. Physiol. Cell Physiol.* In press.
22. Akeson, M., D. Branton, J. J. Kasianowicz, E. Brandin, and D. W. Deamer. 1999. Microsecond time-scale discrimination among polycytidylic acid, polyadenylic acid, and polyuridylic acid as homopolymers

or as segments within single RNA molecules. *Biophys. J.* 77:3227–3233.

23. Kasianowicz, J. J., E. Brandin, D. Branton, and D. W. Deamer. 1996. Characterization of individual polynucleotide molecules using a membrane channel. *Proc. Natl. Acad. Sci. USA.* 93:13770–13773.
24. Henrickson, S. E., M. Misakian, B. Robertson, and J. J. Kasianowicz. 2000. Driven DNA transport into an asymmetric nanometer-scale pore. *Phys. Rev. Lett.* 85:3057–3060.
25. Song, L., M. R. Hobaugh, C. Shustak, S. Cheley, H. Bayley, and J. E. Gouaux. 1996. Structure of staphylococcal alpha-hemolysin, a heptameric transmembrane pore. *Science.* 274:1859–1866.
26. Montal, M., and P. Mueller. 1972. Formation of bimolecular membranes from lipid monolayers and a study of their electrical properties. *Proc. Natl. Acad. Sci. USA.* 69:3561–3566.
27. Colombini, M. 1987. Characterization of channels isolated from plant mitochondria. *Methods Enzymol.* 148:465–475.
28. Freitag, H., R. Benz, and W. Neupert. 1983. Isolation and properties of the porin of the outer mitochondrial membrane from *Neurospora crassa*. *Methods Enzymol.* 97:286–294.
29. Colombini, M., C. L. Yeung, J. Tung, and T. Konig. 1987. The mitochondrial outer membrane channel, VDAC, is regulated by a synthetic polyanion. *Biochim. Biophys. Acta.* 905:279–286.
30. Mangan, P. S., and M. Colombini. 1987. Ultrasteep voltage dependence in a membrane channel. *Proc. Natl. Acad. Sci. USA.* 84:4896–4900.
31. Rostovtseva, T. K., N. Kazemi, M. Weinrich, and S. M. Bezrukov. 2006. Voltage gating of VDAC is regulated by nonlamellar lipids of mitochondrial membranes. *J. Biol. Chem.* 281:37496–37506.
32. Zizi, M., L. Thomas, E. Blachly-Dyson, M. Forte, and M. Colombini. 1995. Oriented channel insertion reveals the motion of a transmembrane beta strand during voltage gating of VDAC. *J. Membr. Biol.* 144:121–129.
33. Li, S. K., A. H. Ghanem, C. L. Teng, G. E. Hardee, and W. I. Higuchi. 2001. Iontophoretic transport of oligonucleotides across human epidermal membrane: a study of the Nernst-Planck model. *J. Pharm. Sci.* 90:915–931.
34. Cui, S. T. 2004. Molecular dynamics study of single-stranded DNA in aqueous solution confined in a nanopore. *Mol. Phys.* 102:139–146.
35. Mannella, C. A., M. Forte, and M. Colombini. 1992. Toward the molecular structure of the mitochondrial channel, VDAC. *J. Bioenerg. Biomembr.* 24:7–19.
36. Cescatti, L., C. Pederzolli, and G. Menestrina. 1991. Modification of lysine residues of *Staphylococcus aureus* alpha-toxin: effects on its channel-forming properties. *J. Membr. Biol.* 119:53–64.
37. Xu, X., J. G. Forbes, and M. Colombini. 2001. Actin modulates the gating of *Neurospora crassa* VDAC. *J. Membr. Biol.* 180:73–81.
38. Colombini, M. 1987. Regulation of the mitochondrial outer membrane channel, VDAC. *J. Bioenerg. Biomembr.* 19:309–320.
39. Mannella, C. A. 1989. Structure of the mitochondrial outer membrane channel derived from electron microscopy of 2D crystals. *J. Bioenerg. Biomembr.* 21:427–437.
40. Florke, H., F. P. Thinnes, H. Winkelbach, U. Stadtmuller, G. Paetzold, C. Morys-Wortmann, D. Hesse, H. Sternbach, B. Zimmermann, P. Kaufmann-Kolle, M. Heiden, A. Karabinos, S. Reymann, V. E. Lalk, and N. Hilschmann. 1994. Channel active mammalian porin, purified from crude membrane fractions of human B lymphocytes and bovine skeletal muscle, reversibly binds adenosinetriphosphate (ATP). *Biol. Chem. Hoppe Seyler.* 375:513–520.